Designing a Test System to Evaluate the Power Conversion Efficiency of

Nanofluidic Pressure-to-Potential (nanoP2P) Converters

Undergraduate Honors Thesis

Presented in Partial Fulfillment of the Requirements for

Graduation with Honors Research Distinction in Mechanical Engineering at

The Ohio State University

April 2015

by

Molly Marie Bennett

Advisor: Shaurya Prakash, Ph.D.

ABSTRACT

Nanofluidic pressure-to-potential converters, nanoP2P converters, are a possible clean source of energy that could reduce the United States' consumption of fossil fuels by harvesting waste pressure to generate usable electrical potential. As envisioned, nanoP2P converters would collect waste pressure from movement, such as traffic or an individual's walking motion, and apply it over a bank of nanochannels filled with ionic solution. The pressure-driven flow of ions through the nanochannels generates a streaming potential that can be harnessed as electrical power. Prior research on nanoP2P converters with induced fluidic slip determined a theoretical maximum power conversion efficiency of 70%, however, the greatest reported efficiencies of devices without slip are only around 1%.

The objectives of this project are to conduct case studies to assess the theoretical feasibility of nanoP2P converters in real-world applications and to design and implement a testing system that will apply 85 psi from a compressed air valve to simulate the waste pressure streams that would be found in the projected end-use. This research demonstrates that nanoP2P converters can feasibly supplement up to about 50% of the electricity consumption of streetlights in optimal conditions. However, this technology does not seem appropriate for supplementing the power of traffic lights at large intersections. In the case of using nanoP2P converters to power personal devices from human movement, theoretical percentages of smart phone consumption were much less than one percent, meaning this application is not feasible either. In the assembled test setup, tubing runs from a compressed air source to a T-connector sealed to a device fabricated in the Microsystems and Nanosystems Laboratory. Epoxy was used to seal the T-connector to the device, however this method seems to yield varying results. Streaming potential data has not been collected due to leaky connections at the T-connector base.

ACKNOWLEDGEMENTS

Many people contributed to the success of this project. First, I would like to thank my advisor, Dr. Shaurya Prakash, for serving as my mentor while I completed this research project. He has kept me focused on the important objectives for my research, while presenting numerous beneficial research and career opportunities to me. It has been great to have the guidance of such a supportive and motivating individual throughout my research project. I am so thankful for his insight, knowledge, and contributions to my work. I look forward to working with Dr. Prakash as I pursue my Master's in Mechanical Engineering.

I would like to thank Dr. Emily Rosenthal-Kim for providing feedback whenever I needed assistance. She kept me focused on deadlines and provided me with a different perspective on my work. I am so grateful for her contributions to my presentations, proposal, and thesis. I would also like to thank Kaushik Rangharajan for serving as my graduate mentor within the lab. He provided me with great feedback and suggestions throughout the entire process and brought all areas of concern to my attention. He also helped me order components, build my test setup, and collect data. He has been very helpful and willing to spend time with me to help solve any issues I was having. I would also like to thank Marie Fuest and Caitlin Boone for offering suggested solutions and helping me make secure connections in my system.

I would like to thank the Microsystems and Nanosystems Lab group for their support and constructive criticism throughout our lab meetings and my presentations. It is great to have input from various perspectives and backgrounds to help frame a talk appropriately for the audience. In conclusion, I would like to thank my family, friends, and boyfriend for supporting me and balancing out the nonacademic half of my life throughout my entire college career. I am so lucky to have equally motivating, encouraging, and supportive personal and professional networks.

TABLE OF CONTENTS

LIST OF FIGURES

CHAPTER 1: INTRODUCTION

In 2013, the United States generated 4 trillion kilowatt-hours of electricity, of which 67% was generated from the burning of fossil fuels [1]. Nanofluidic pressure-to-potential converters, nanoP2P converters, are a possible source of energy harvested from available waste pressure streams that could enhance process efficiency in many domains and therefore help reduce the United States' consumption of fossil fuels by generating usable electric potential difference. For example, traffic lights, streetlights, and highway lights consume approximately 32 billion kilowatt-hours of electricity annually, a significant cost that could be reduced by a clean, alternative source of energy [2,3]. As envisioned, nanoP2P converters would collect waste pressure from local movement, such as traffic passing through an intersection or an individual's walking motion, and apply it over a bank of nanochannels filled with ionic solution.

Another application of this technology could be to use the device as a highly sensitive pressure sensor. The expected output voltage of a single nanoP2P converter is in the range of 1 nv to 1 mV. For every change in input pressure, a different voltage would be collected across the reservoirs. This small measured voltage could be calibrated to correspond to given input pressure. This device could be implemented in various applications to sense changes in pressure with very small resolution.

1.1 Background on Energy Solutions

Energy consumption is dominated by non-renewable sources in the United States. Only 17.9% of energy came from renewable sources in 2013 [1]. The breakdown of energy consumption by source in the United States in 2013 can be found in Figure 1. Of the total energy consumed in 2013, 13.8% of resources were used to generate electricity [1]. The renewable sources that contribute a significant amount of energy available for subsequent use and consumption in the

US include hydroelectric power, biomass, wind energy, geothermal power, and solar energy [1]. Wind, water, and solar photovoltaic energy are dependent on climate and surroundings and are not suitable for all scenarios. Biomass requires the consumption of other resources to create a reusable product thereby reducing its overall efficiency. A depiction of the cycle to create biodiesel energy from the sun, plants, and crop refinement as well as the production of biodiesel is shown in Figure 2.

U.S. Energy Consumption 2013

Natural Gas 27.3%

Nuclear 8.5%

Hydroelectric 2.8%

Coal 18.3%

Biomass 4.6%

Wind 1.4%

Geothermal 0.4%

Solar 1.4%

Petroleum 18.3%

Source: Institute for Energy Research
Monthly Energy Review, April 2013
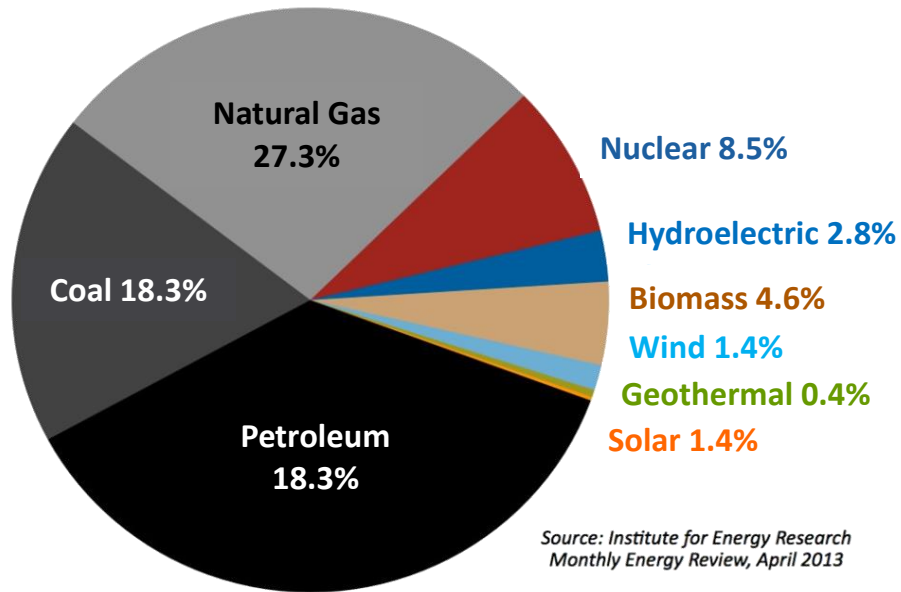
Figure 1: Breakdown of US energy consumption by source in 2013 [3]
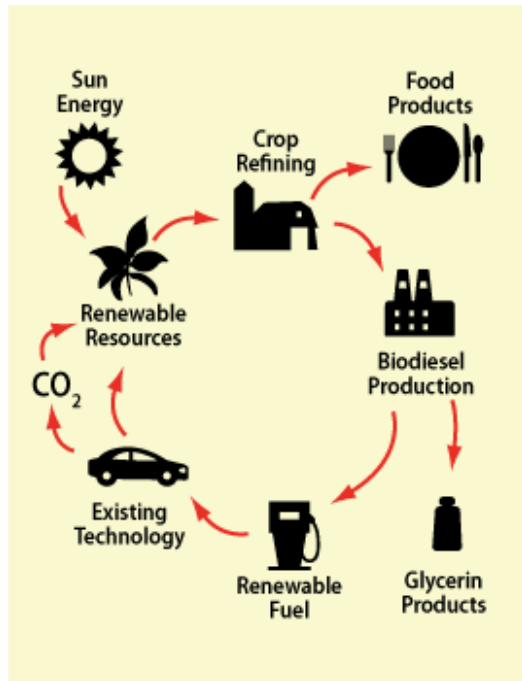
Figure 2: Biodiesel cycle [5]

NanoP2P converters will serve to supply clean energy that utilizes waste pressure from other sources to provide power to the overall energy efficiency of a process. Waste pressure can be collected from various existing behaviors and operations, as will be explored later in this thesis. By collecting waste pressure from an energy consuming process, the process becomes more efficient and nanoP2P converters are able to supply voltage directly to power operations without consuming significant additional resources during energy conversion.

1.2 Background on Nanofluidic Pressure-to-Potential Converters

There are a few key components that characterize nanoP2P converters. The first component is the dimensions of the channels used to transport fluid. As the name would suggest, nanofluidic pressure-to-potential converters utilize nanochannels to transport ionic solution. A nanochannel is defined as a hollow channel with at least one dimension of its cross-section in the 1–100 nm range [6]. For nanoP2P devices, the height is typically the dimension on the nanoscale, while the

3

width and length are greater. A diagram labeling the locations of these dimensions can be found in Figure 3. For the purpose of this research, the height of the nanochannels is on the order of 1–100 nm, the width is in the order of 1–100 μm, and the length is on the order of 1–100 mm. It is worth noting, as shown later, that the nanochannel geometry is a design parameter that can be optimized for highest efficiency in conversion of pressure to potential.
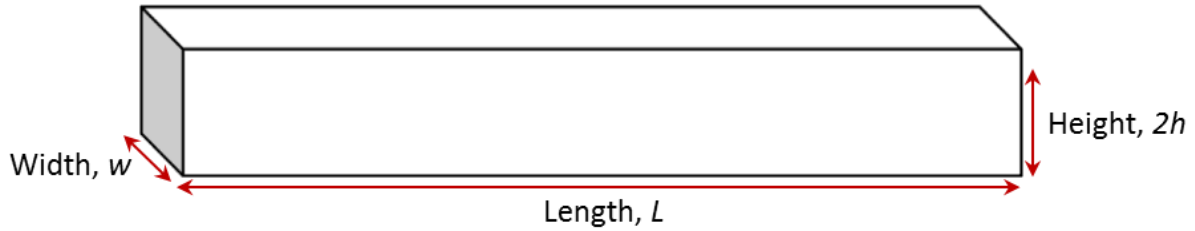
Figure 3: Nanochannel dimensions

An example of a simple nanofluidic device and its data collection system is presented in Figure 4. Figure 4a shows a single nanochannel with a width of 50 μm running between the input and output reservoirs of the device. Figure 4b demonstrates the high-pressure air source connected to the input reservoir and lead wires connected to both reservoirs and a voltmeter to measure the voltage generated in the system. In a real application of this device, the voltage collected from the output would be stored in a bank of capacitors until it was used as electricity by another source.
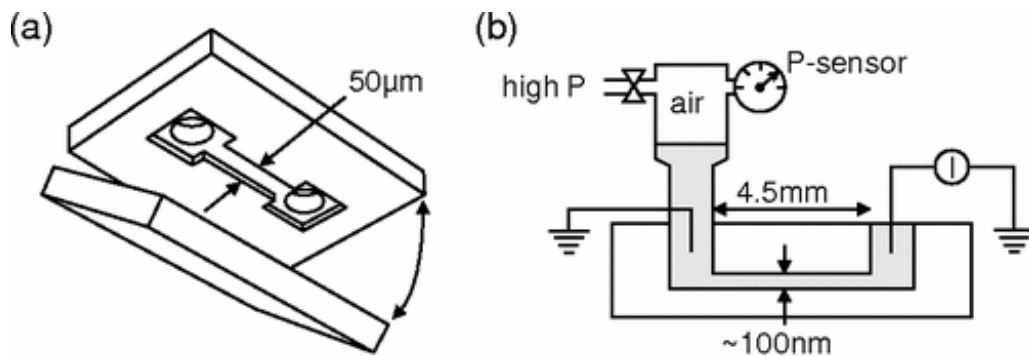
Figure 4: Simple nanoP2P converter and data collection system reported previously [10].

The second characterization of nanoP2P converters is the mode for direct energy conversion. High pressure is applied to the device and converted into an electric potential that can be collected from the output and used as electricity. More specifically, high pressure is applied to the input reservoir of the nanoP2P converter device and forces an ionic solution through a nanochannel or bank of nanochannels connected in parallel. The pressure-driven flow of ions through the nanochannels creates a streaming current inside the channels [10]. The system develops a streaming potential downstream in order to counteract the streaming potential inside the channels. This streaming potential or voltage is the output of the system, and the change in voltage is collected between the input and output reservoirs.
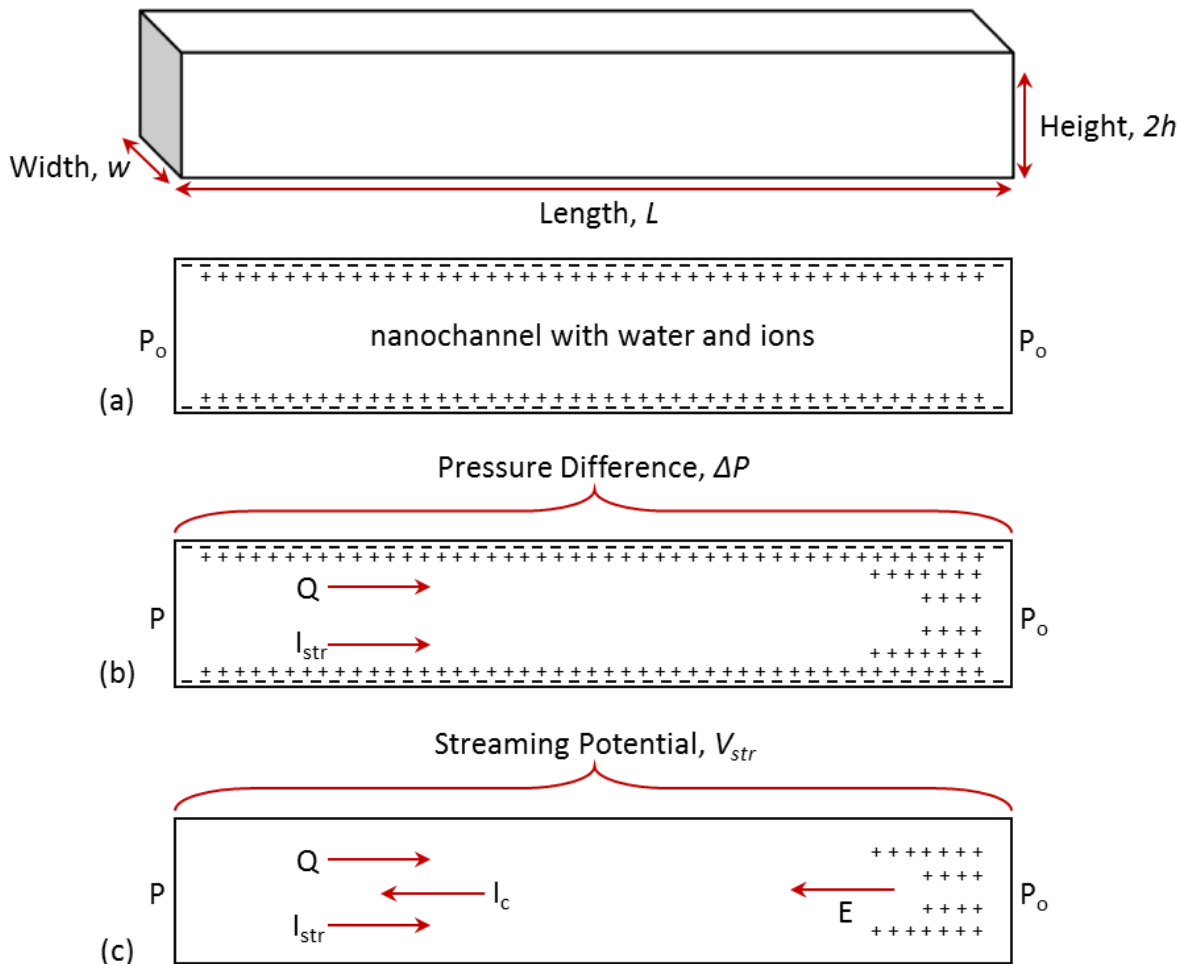
Figure 5: Transport of charge inside a nanochannel

The forced flow of positive ions in the diffuse layer past the shear plane near the wall generates a streaming potential across the channel, as depicted in Figure 4, an adaptation from Olthius *et al.*, *Sensors and Actuators B*, 2005. In the figure, P_o represents atmospheric pressure, P represents applied pressure, and Q represents volumetric flow. In Figure 5a, both ends of the channel are open to atmospheric pressure and the ions remain still inside the channel. The positively charged ions of the solution are attracted to the negative surface charge of the glass substrate. In Figure 5b, the pressure difference between the two ends of the channel causes the ions to flow toward lower pressure. Streaming current, I_{str}, is generated inside the channel from the pressure-driven flow of positively charged ions along the walls of the channel. The gradient in concentration of ions along the length of the channel causes an electric field, E, shown in Figure 5c. The electric field causes a change in potential over the length of the channel, V_{str}.

$$\varepsilon_{tot} = \frac{P_{ext}}{P_{hydro}} = \frac{I_{str}V_{str}}{\Delta P Q} \tag{1}$$

$$v_x = \frac{-h^2 \Delta P}{2\mu L}\left[\left(1 - \left(\frac{z}{h}\right)^2\right) + \frac{2b}{h}\right] \tag{2}$$

$$Q = \int_{0}^{w}\int_{-h}^{h} v_x \, dz \, dy = \frac{-2wh^2\Delta P}{3\mu L}[h + 3b] \tag{3}$$

$$\frac{Q_{slip}}{Q_{no\ slip}} = \frac{h + 3b}{h} = 1 + \frac{3b}{h} \tag{4}$$

NanoP2P converters are evaluated for effectiveness by power conversion efficiency, ε. The expression for this efficiency is included above in Equation 1, where P_{hydro} is the hydrodynamic power and P_{ext} is the power dissipated in the external load [9]. The pressure gradient between the input and output reservoir is denoted as *ΔP*. The energy conversion efficiency can be improved by altering the surface properties of the substrate to make the surface

more hydrophobic and to adjust the surface charge density. A hydrophobic surface engineers slip into the system to promote velocity of the ions at the walls of the channel. The expression for the velocity profile through a channel with a rectangular cross section is given above in Equation 2. Flow rate is determined by taking the double integral of the expression for the velocity profile with respect to the direction of the channel width and the direction of the channel height, y and z, respectively. Flow rate is dependent upon the dimensions of the channel and the expression for the slip condition is listed above in Equation 3, where μ is the kinematic viscosity of the fluid and b is the slip length. The expression for flow rate in the no slip condition is obtained by substituting in a slip length of zero into Equation 3. The ratio relating the slip flow rate with the flow rate in the no slip condition is included in Equation 4.

These expressions for flow rate are 2D approximations with the flow rate profile represented in the *x-z* plane where the x-axis is along the channel length and the z-axis is along the channel height. The flow rate equation has a negative sign because the pressure at the outlet is lower than the pressure at the inlet, yielding a negative *ΔP*. The no slip condition states that the velocity of the fluid boundary is equal to that of the velocity of the solid boundary, or channel wall. The slip condition means that the velocity of the fluid is no longer equal to that of the solid at the boundary. The amount of slip in the system is characterized by the slip length. To measure the slip length, the channel walls are shifted in the flow field to meet the condition that the fluid velocity is the same as the velocity of the wall, as demonstrated in Figure 6.
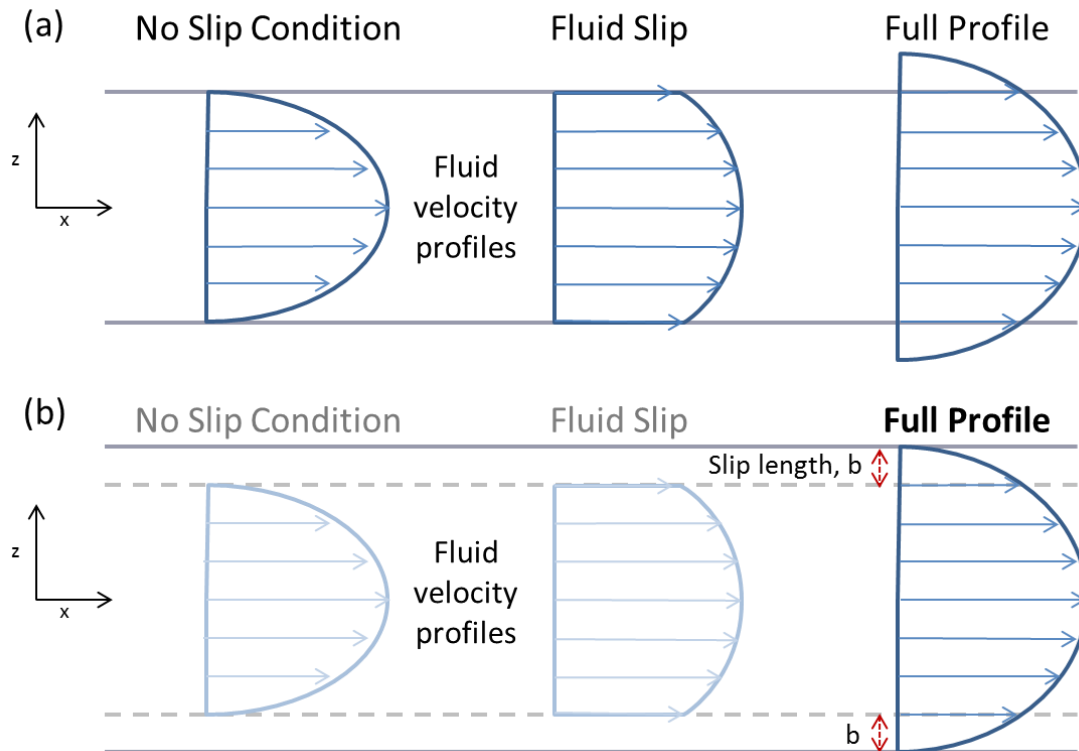
Figure 6: 2D representation of slip in a channel

1.3 Problem Statement

The first objective of this research is to conduct two theoretical case studies to determine the feasibility of this technology. The second objective of this research is to design, build, and test a reliable system that applies high pressure and collects a voltage from a micro- or nanofluidic device.

1.4 Significance of Research

This project will allow the Microsystems and Nanosystems Laboratory to test nanoP2P converters and analyze their performance for energy conversion efficiency. With a reliable test setup and data collection system, the lab can work toward reaching and surpassing the state-of-the-art in the field. This research also serves to analyze the feasibility of this technology in a few

scenarios. Further case studies should be performed, however this research examines a few initial applications for this technology.

NanoP2P converters could benefit society in two ways: by reducing consumption of fossil fuels and by improving the efficiency of current processes. Fossil fuel consumption could be reduced by nanoP2P converters because significantly less fossil fuel resources would be needed to produce and operate the devices compared to other forms of energy, such as coal, natural gas, and petroleum. NanoP2P converters would also serve to improve the efficiency of current technologies by collect waste pressure from motion in the surrounding areas. For instance, nanoP2P converters could collect waste pressure from cars driving through an intersection and convert that energy into electricity that could be stored in capacitor banks to help power street- and traffic lights. NanoP2P converters could also be implemented in the soles of running shoes to collect pressure from the impact of a person's shoe with the ground while walking and running. The devices would be placed so that the input reservoirs to the nanofluidic devices would be placed in the locations that experience the highest pressure in the shoes. This energy could then be converted into electricity, stored in capacitors embedded in the shoes, and used to help charge a cell phone.

1.5 Overview of Thesis

This thesis contains four chapters: Introduction, Methodology, Results and Discussion, and Conclusions and Future Work. Chapter 2 discusses the methodology used to analyze case studies and design the test setup. Chapter 3 presents the results from the case studies as well as the final test setup and data reflecting its reliability. Chapter 4 reflects on the research presented and discusses future work to be conducted on this research topic.

In the following chapters two case studies are presented that analyze the feasibility of nanoP2P converters as a source of electricity in two different scenarios. The first case study looks at embedding thousands of nanoP2P converter devices into traffic intersections to collect pressure from vehicles driving through the intersection and therefore over the devices. The second case study evaluates embedding nine devices into the soles of running shoes to collect pressure from the applied force of individuals walking and running in the shoes and therefore on the devices. These case studies will compare the energy expenditures of current technologies against the implementation of nanoP2P converter devices to characterize each case study as feasible or not feasible.

The second component of this thesis involves setting up a leak-free system that applies a high pressure to the input reservoir and collects a voltage from the output reservoir. It is important to demonstrate the reliability of the system so that nanoP2P converters can be accurately analyzed for power conversion efficiency. This thesis will present the rationale for the nanoP2P system with example case studies and the design, implementation, and results of the test setup.

CHAPTER 2: METHODOLOGY

In this chapter, the proposed solution will be presented and analyzed in two different case studies. The system design and implementation will be described and presented at the end of this chapter.

2.1 Proposed Solution

The proposed implementation of this technology is described specifically in the following sections of this chapter. In general, nanoP2P converters could theoretically be implemented as mobile energy generators in various scenarios. The key attributes that limit the implementation of this device are as follows: a need for a high amount of waste pressure to collect as an input and a need for an application that uses low but relatively consistent amounts of electricity throughout the year. The case studies evaluated in this chapter include supplementing power of LED traffic lights or streetlights and charging mobile devices.

Several parameters can be adjusted in the design of nanoP2P converters to yield varying power output results. The first parameters that effect power output are the dimensions of the nanochannels (height, length, and width). These parameters impact the flow rate through the channels. Similarly, slip length increases the flow rate through the channel(s). As demonstrated in Equation 4 earlier, the expressed relating flow rate with and without slip is a function of slip length and one-half the channel height. A graph representing the effects of slip length compared to flow rate is presented in Figure 7, where a half channel height, h, of 50 nm was used and slip length, b, values range from zero to 100 nm. A maximum slip length of 100 nm was chosen because this value seems to be the practical limit on slip length in nanochannels of a 100 nm depth.
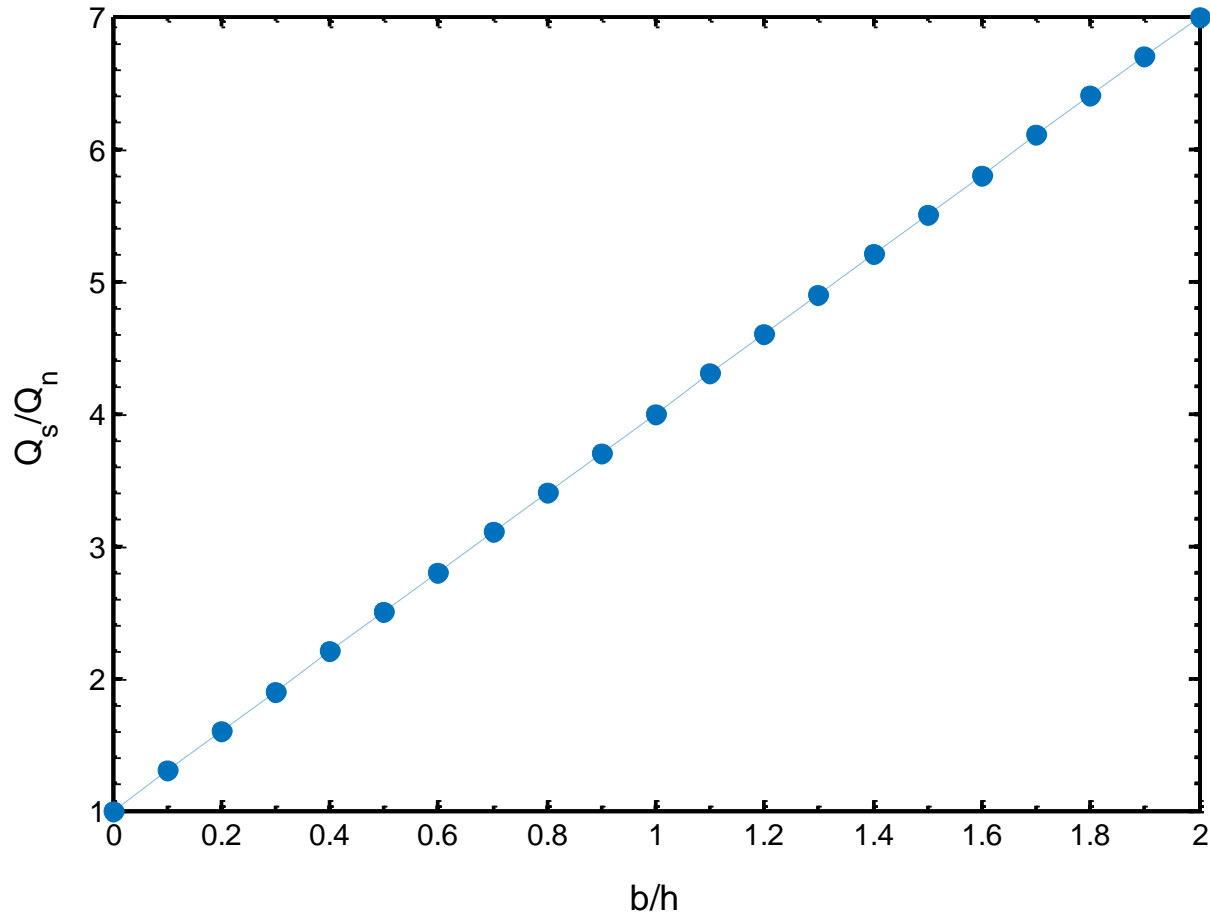
Figure 7: Effect of the ratio of slip length to half channel height on flow rate

The next factor that impacts power output is the number of channels connected in parallel. As the number of channels increases, the flow rate through the system increases by a factor of *n*. The pressure gradient across the channels drives the flow rate through the system, however is also impacts the power output of the device. The power conversion efficiency dictates how much input energy is actually converted into usable electric energy, and is determined based on the input flow rate and pressure and output streaming potential and current. However, for this purpose of this study, the power conversion efficiency is treated as a control variable to study the effects of channel dimensions on flow rate and power output and to simplify calculations. The list of control variables is included below in Table 1.

Table 1: Design parameters

Variable	Meaning
$H = 2h$	Channel Height
w	Channel Width
L	Channel Length
n	Number of Channels in Parallel
ΔP	Pressure Gradient across Channels
ε	Power Conversion Efficiency

A preliminary design for a nanoP2P device was created in order to evaluate a these case studies. A simple schematic representing this design is presented below in Figure 8. The device consists of two circular reservoirs, measuring 5 mm in diameter each. The reservoirs will contain the ionic solution to be forced through the bank of nanochannels. The red horizontal lines in the figure represent the nanochannels. For simplicity only a few channels are shown, however each device will contain a bank of 100 nanochannels in parallel for the transport of ionic solution. Each nanochannel is rectangular in cross section with a height of 100 nm and a width of 30 μm. The length of each channel is approximately 1 cm.
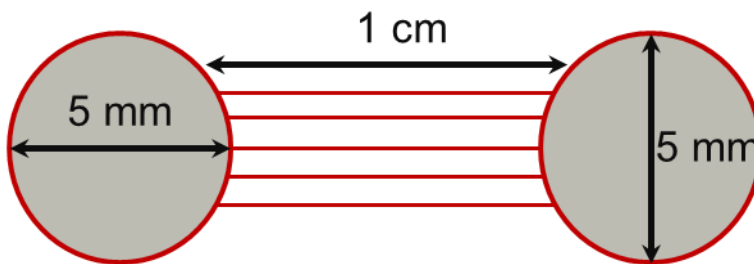

Figure 8: Preliminary device design showing reservoir size and layout

This device design will be used in the following case studies to collect pressure and convert this energy into streaming potential to perform electrical work as indicated in each application. For the purpose of this thesis, the dimensions of the channels are fixed and the

control variables that are altered in each case study are input pressure, slip length, and power conversion efficiency. The fluid in the channels is assumed to have the same dynamic viscosity as water at room temperature, 1.002×10^{-3} N-s/m^2. For the applications using fluid slip, the slip length was assumed to be 100 nm, the practical maximum obtainable slip length in a 100 nm deep channel.

2.2 Case Study I: LED Lighting

Two applications will be explored regarding LED lighting. The first uses nanoP2P converters to power traffic lights. The second application would use nanoP2P converters to power streetlights. These applications are very similar and therefore they are group together in a single case study analysis. In both examples, nanoP2P converters would be embedded under the road to collect waste pressure from cars driving over the devices. The applications will be explained further below.

There are an estimated 300,000 traffic lights in the United States [10]. Most traffic lights use incandescent halogen bulbs, however city-wide replacements in favor of LEDs have started all over the nation. Most traffic lights currently use 100 W incandescent halogen bulbs, however they are being replaced with 15 W LEDs which emit a comparable amount of light while consuming less energy. For this case study analysis, all traffic lights will be assumed to have three 15 W LEDs. Under these assumptions, 300,000 15 W LED traffic lights operating all day everyday consume 39.42 million kW-hr annually. This consumption accounts for 0.001% of the energy generated in 2013. Although this is a small amount of the total energy generation, this case study will still be analyzed to help determine the most appropriate application of this technology.
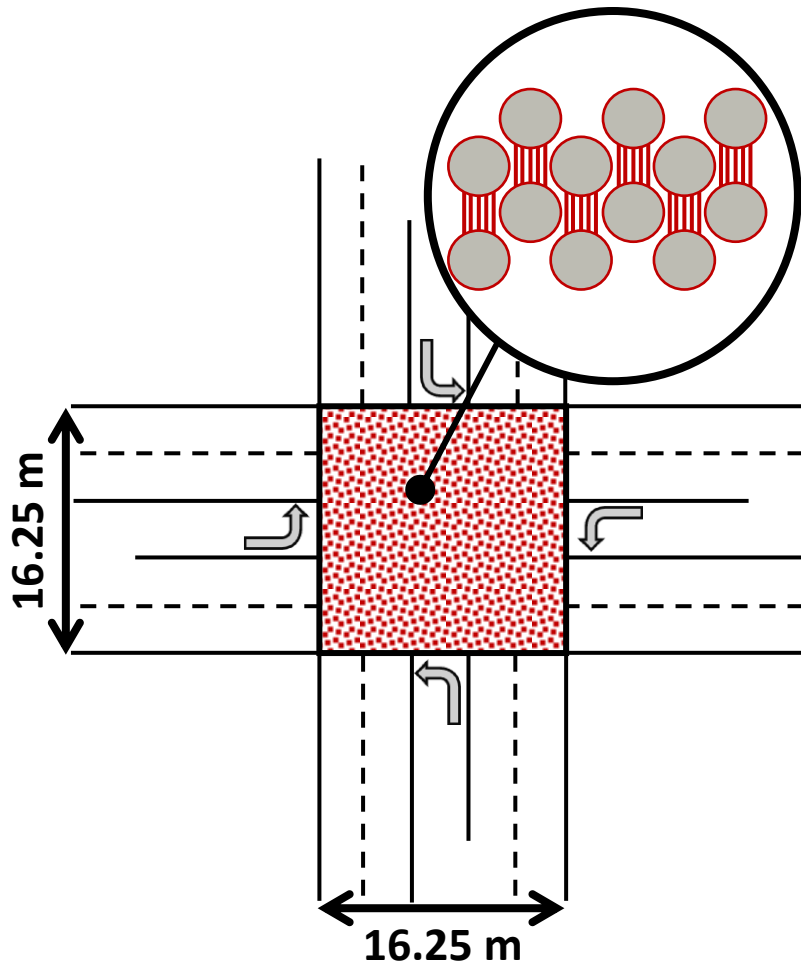
Figure 9: Traffic light case study setup

The setup for this application is briefly mentioned below; however, it will be described in further detail in the next chapter. A five-lane intersection with twelve traffic lights will be the focus of this study. The intersection would have two lanes of traffic driving in each direction and a left hand turn lane for each direction. The setup of this application can be seen in Figure 9. The dimensions of this five-lane intersection are 16.25 m × 16.25 m, where each lane is 3.25 m wide.

In the case of the second LED lighting application, there are an estimated 26 million streetlights in the United States [3]. Most streetlights use high-pressure sodium bulbs, but again these are being replaced by more efficient LED lights. Since LEDs rated at only 25 W each are replacing 100 W HPS bulbs, all streetlights in the case study will be assumed to have one 25 W

LED each. The setup of this analysis is similar to the traffic light case, where a 16.25 m × 16.25 m area of devices would be embedded under a five-lane road near a streetlight. One key difference between streetlights and traffic lights is that streetlights are only producing light from dusk to dawn daily. Therefore, streetlights have a shorter operating time, totaling to about 4100 hours of use per year [11]. All power from the nanoP2P devices embedded in the intersection would go toward the single streetlight instead of being divided among twelve different lights. In this example, under the assumptions made above, LED streetlights consume 2.67 billion kW-hr annually, equaling about 0.067% of the electricity generated in 2013.

2.3 Case Study II: Personal Devices

Smart phones and personal devices are owned by more and more individuals in the United States every year. There were approximately 144.5 million smart phones in use in the United States in 2013 [12]. This posed the question as to how much energy this technology was using, and if the needed electricity to charge these devices could be supplied by nanoP2P converters from waste pressure of human movement. For example, devices could be embedded in the soles of shoes to collect pressure from the impact of the feet contacting the ground during walking and running.

One study compared the energy consumption of the iPhone 5 to the Samsung Galaxy S III and noted that the consumption by smart phones is small compared to that of desktop computers and even laptops [13]. This study stated that the iPhone 5 consumes 3.5 kW-hr annually to charge the device, while the Galaxy S III consumes 4.9 kW-hr annually [13]. This difference in consumption can partially be explained by the size of the phone, and in turn, the size of the battery. The iPhone 5 has a screen size of 4 inches diagonally, with 1136 × 640 pixels [14]. The Samsung Galaxy S III has a screen size of 4.8 inches diagonally, with 1280 × 720 pixels [15]. As the area of the screen increases, a larger battery is needed and this means more energy is used to

charge the phone annually. Since the current trend in smart phone is an increasing screen area, for the purposes of this study all smart phones were assumed to consume 4.9 kW-hr annually to match the larger screen area. When taking these assumptions into consideration, 144.5 million smart phones each consuming 4.9 kW-hr annually, smart phones consume 708 million kW-hr annually, or approximately 0.018% of the electricity generated in 2013. Although this is not a large fraction of the energy generation in the US, this case study was still explored to see if individuals could power their own personal devices.

In this case study, nanoP2P converters were embedded into the sole of a running shoe and positioned in such a way so that the concentration of an individual's weight will be applied to the input reservoirs of nine devices. A schematic of an energy generating running shoe is shown below in Figure 10, where the red reservoirs feel the concentrated force of the runner's feet and are considered the input reservoirs to the devices. In this case study, it will be assumed that as in individual is walking or running, the heel of one foot and the toe of the opposite foot will be in contact with the ground at the same time, such that pressure is always supplied to 9 devices at a time. One study at Harvard determined that as a person walks, the force he or she exerts is 1.5 times that of their body weight, and three times while running [16]. This difference in force determines the difference in the results for the walking and running cases as presented in the next chapter.
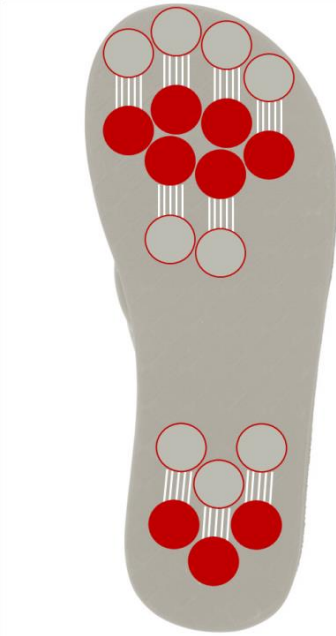
Figure 10: Running shoe with embedded devices

2.4 System Design and Implementation

As the next phase of this project, a test setup for evaluating nanoP2P converters was designed and then implemented in the lab. The main factors that limited the design of this system were the high pressure input, streaming potential output, and available resources in the Microsystems and Nanosystems Laboratory. The first stage of design involved determining the types of components that were needed in order to achieve the necessary operations: applying a high pressure input and measuring a voltage output. The pressure source selected was compressed air because it would be readily available in the laboratory, easy to access, and simple to control. In order to deliver the compressed air to the system, high pressure tubing was needed along with air-tight connections. The chosen means to attach the device to the tubing was a connector that was mounted on the device over the input reservoir. This connector also needed to allow access to measure the voltage at the input reservoir, however. Lead wires and a voltmeter would be used

to collect voltage from the reservoirs to test for reliability of the system. Based on previously reported research within the field, the voltages read from the system were expected to be on the order of 1 to 100 nV, so a Faraday cage would be needed in order to help reduce noise in the voltage readings resulting from outside sources.

The first iteration of the test setup design is presented in Figure 11. This design consisted of compressed air supplied at 85 psi located near the ceiling in the lab. Since this valve would be inconvenient to access, a needle valve was included to be able to apply and remove the pressure from the system. After the needle valve, tubing connected to a T-connector so that voltage could be read from the side arm while high pressure was delivered through the vertical portion of the connector. Please note that the device depicted in the following figures is not to scale, but shown larger for detail. The blue shading represents ionic solution in the reservoirs and nanochannel.
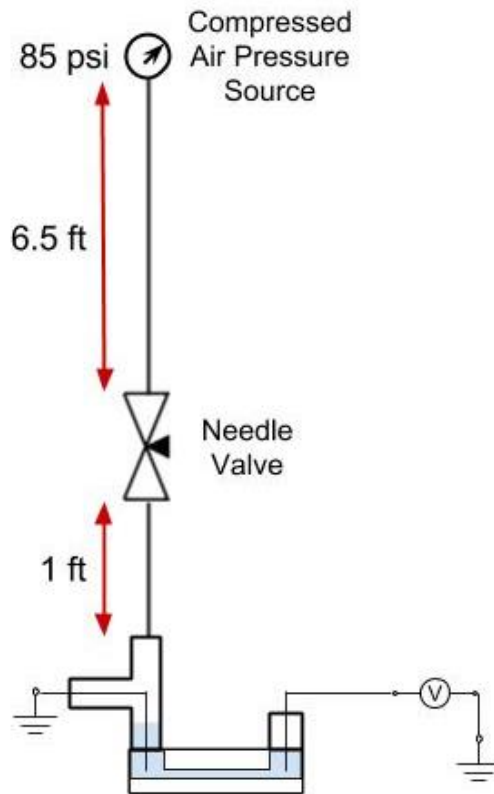

Figure 11: Preliminary test station design

This preliminary design was not ideal because the needle valve would reduce the amount of pressure supplied to the input reservoir and we would have more tubing and connections than necessary. A new design was created after a different compressed air valve became available in the lab that was accessible from ground level. Based on the locations of this compressed air source and the Faraday cage in the lab, the setup would need to look similar to the schematic shown in Figure 12.
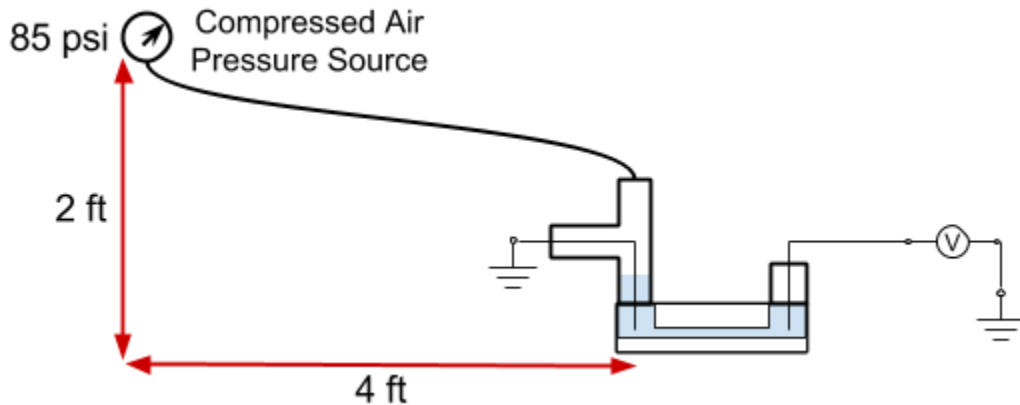

Figure 12: Simple schematic of final test station

In this schematic, the basic components of the system are shown. The first is the high pressure compressed air source at 85 psi, controlled by the built-in pressure regulator. The value for the pressure source was chosen to remain consistent with existing research in the field for comparable results in the future. From the compressed air source, tubing runs to a T-connector with leak-free and sturdy connections. This shape of connector was chosen for this design to allow pressure to be supplied through the vertical portion of the connector while the ground voltage could be measured from the arm of the T-connector. In order to apply high pressure and read a consistent voltage, the arm of the connector would need to be sealed completely while still allowing access to the lead wire in contact with the solution in the input reservoir. This posed a challenge in the design process for the test setup, and will be discussed later. Next, the connector

would need to be mounted upright to the device while restricting all leaks. It is also important that no bonding agent seeps into the reservoir while attaching the connector because it could restrict flow through the channels or contaminate the ionic solution. Again, this posed a difficult design challenge. At the output reservoir, a lead wire would need to be in contact with the ionic solution as well, however this reservoir is open to atmospheric pressure.

The search for compatible components began with the available resources in the lab. Operating pressure was one of the main considerations when choosing components because the system cannot leak air or ionic solution, nor can parts fail under the high pressure. Therefore, all chosen components must be rated for pressures above 85 psi. From the lab, compatible high-pressure tubing and a quick connect hose coupling were obtained and incorporated into the test setup. The tubing has an inner diameter of ¼ inch and is reinforced with a polyester braid for strength. Hose clamps were used at the tubing and connector interfaces to ensure leak-free and secure connections. The appropriate T-connectors were chosen based on a pressure rating of 150 psi and barbed style, also to ensure a secure connection. Copper wire was selected to read the voltage difference between the input and output reservoirs in this stage of the project because it is readily available in the lab and will suffice to take measurements to validate a working test setup. A SolidWorks model of the test setup is shown in Figure 13: Model of test setup, with a detailed view of the pressure source and device shown in Figure 14 and Figure 15, respectively.
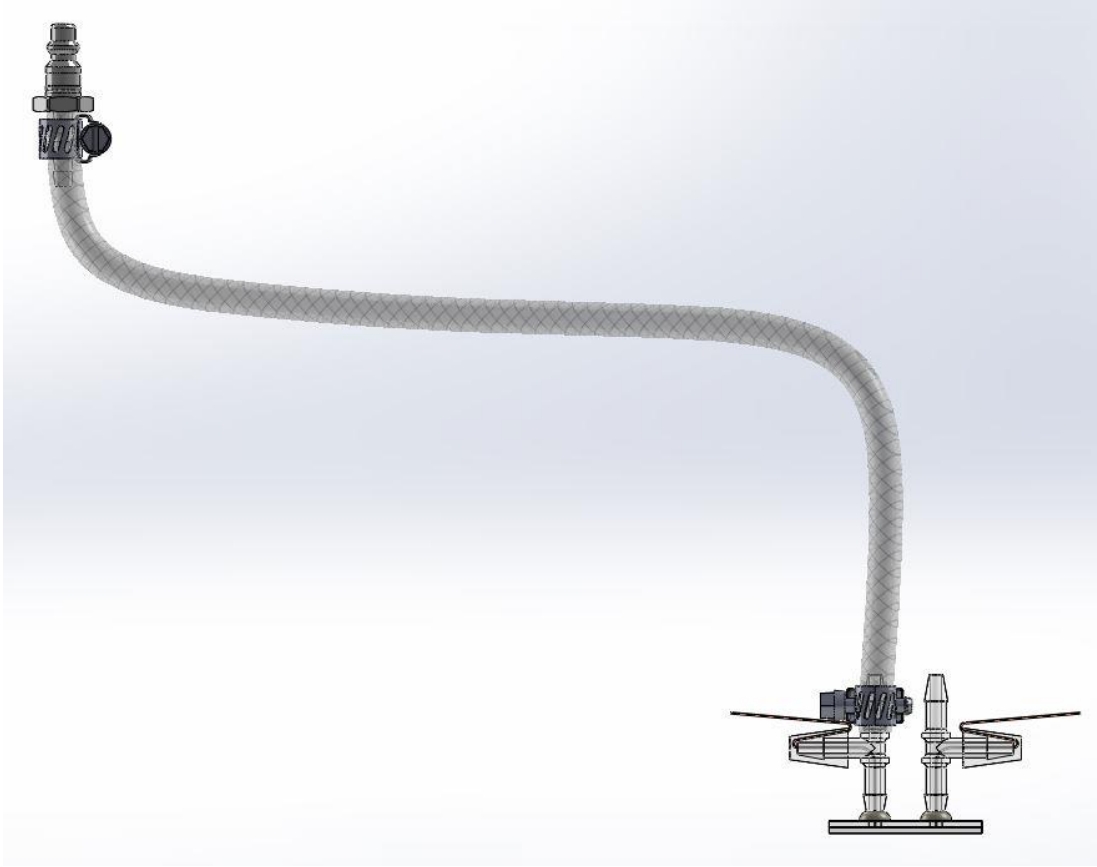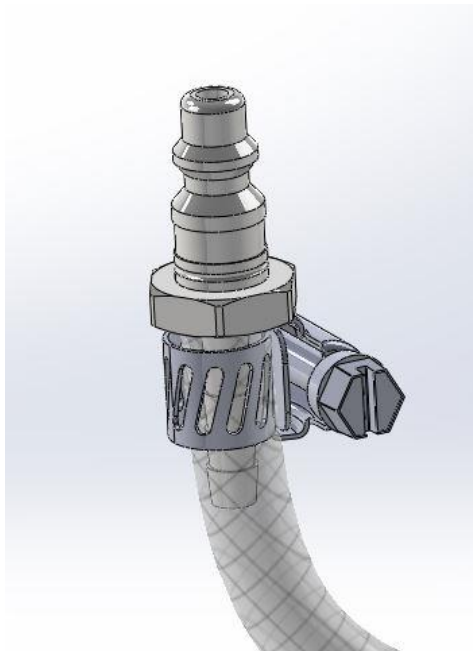
Figure 13: Model of test setup

Figure 14: Detailed view of pressure source input of the test setup model
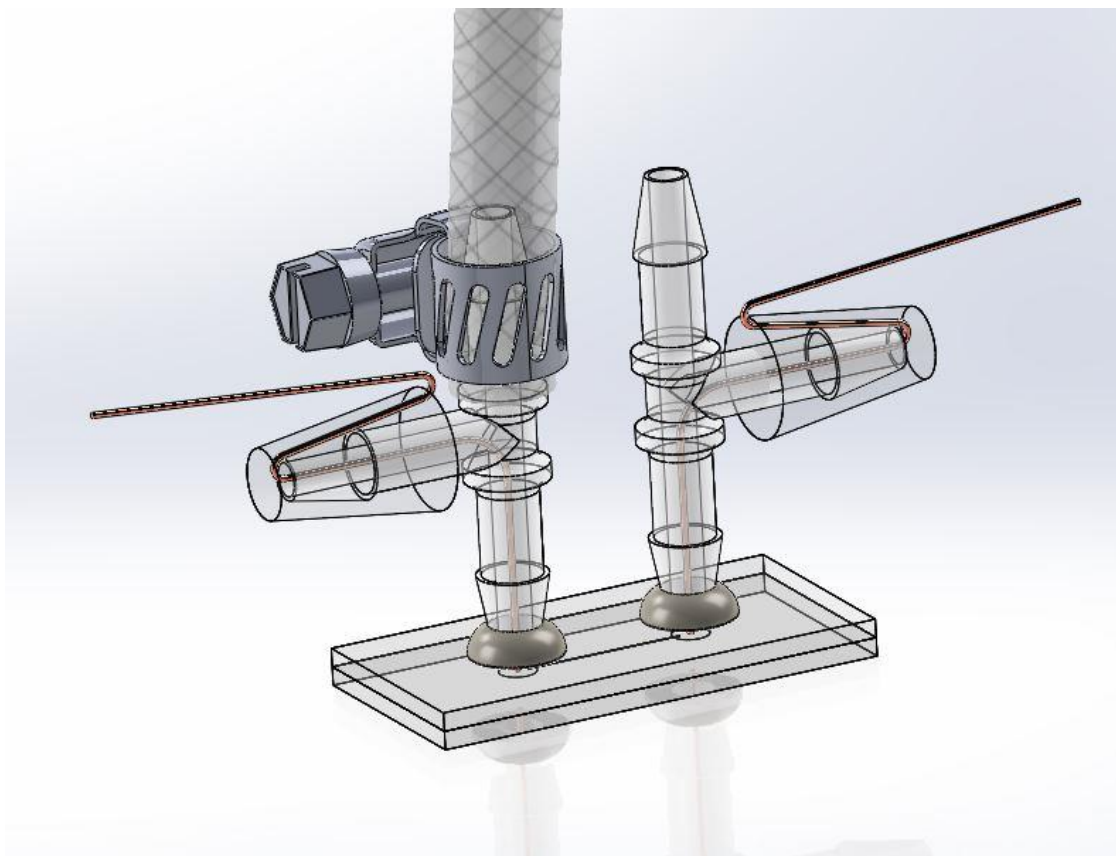
Figure 15: Detailed view of device in the test setup model

After all the major components were selected, the next challenge was to choose the means of sealing the side arm of the T-connector and bonding the base of the T-connector with the devices. The first method discussed to deal the arm was to machine a small metallic piece to fit inside the side arm that would restrict leakage of air. This piece would also need to be in contact with the ionic solution at all times to properly read the voltage from the input reservoir. This method seemed impractical to be able to machine a piece accurate enough to fit inside the tube without leaking air. The final idea, as presented in Figure 16 along with the rest of the setup, was to cap off the side arm with polydimethylsiloxane (PDMS). PDMS starts as a liquid bulk and activator and cure to be a pliable solid. This would allow for control of the shape of the cap and use of lead wires to measure the voltage. The lead wire would run from the input reservoir, in

contact with the ionic solution, up and through the side arm of the T-connector. The lead wire would be stationary and embedded in the PDMS end cap, secured to the connector. To secure the device to the connector, very high peel strength Double Bubble Epoxy was used because it has a high strength rating. The epoxy has a dark gray appearance and can be seen below in Figure 16. Detailed images of the components used in this setup can be found in Appendix A. Furthermore, the reliability of this setup will be assessed in the next chapter. This assessment will relate the input pressure to the output voltage measured across the channel(s).
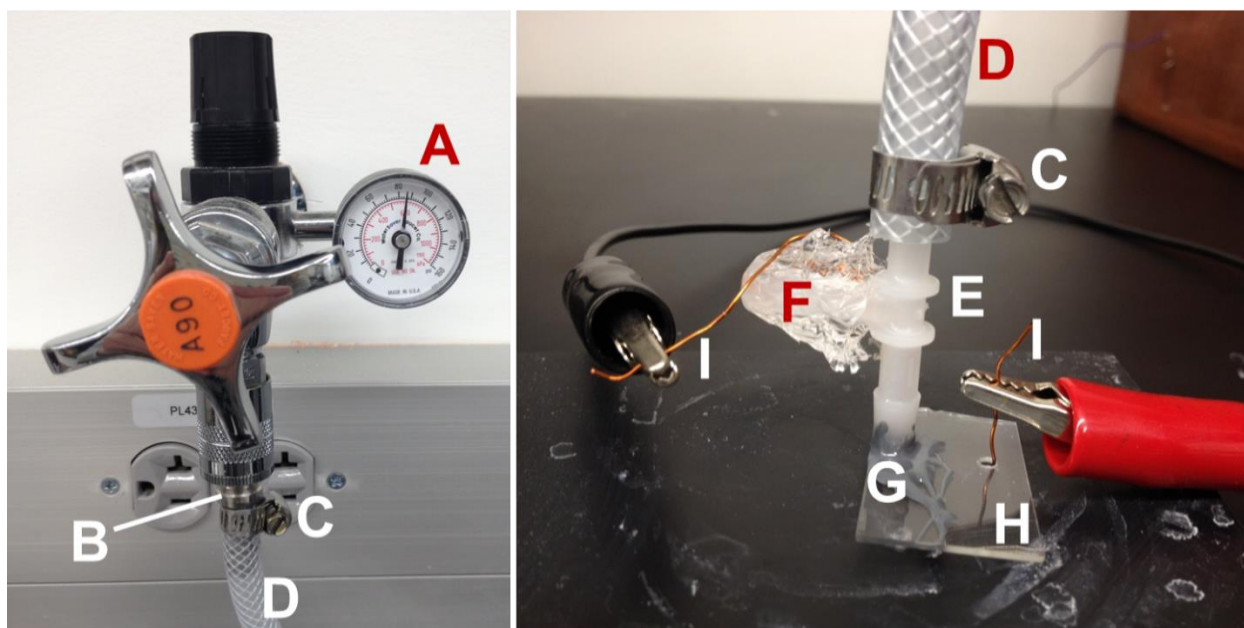
A. Compressed Air, 85 psi   D. Tubing, ID of ¼"   G. Double Bubble Epoxy
B. Hose Coupling   E. T-Connector   H. NanoP2P Device
C. Hose Clamp   F. PDMS Plug   I. Copper Wire

Figure 16: Setup of testing station

CHAPTER 3: RESULTS AND DISCUSSION

The results regarding the case studies and reliability of the test setup are discussed in this chapter. The progression of equations and assumptions used to analyze each case study are presented, followed by a discussion as to what the resulting values mean. The validation process regarding the reliability of the test setup is discussed in the final section of the chapter.

3.1 Case Study I: LED Lighting

In order to evaluate the LED lighting case study, specific assumptions were made about the conditions of operation. It was assumed that each traffic light held three 15 W LEDs, with only one operating at a time throughout the day. Assuming a five-lane intersection, operating year-round, the twelve traffic lights consume 1577 kW-hr of electricity annually, as shown in Equation 5. The next set of assumptions were derived from the traffic conditions and pressure inputs to the devices. Since each device measures 0.5 cm × 2 cm, and the five-lane intersection measures 16.25 m × 16.25 m, 2,640,625 devices can be embedded under the intersection. Again, each device contains 100 nanochannels connected in parallel and 5 mm diameter reservoirs.

$$Consumption = 12\ Lights \times \frac{15\ W}{Light} \times \frac{kW}{1000\ W} \times \frac{24\ hr}{day} \times \frac{365\ days}{yr} = \boldsymbol{1577}\ \frac{\boldsymbol{kW \cdot hr}}{\boldsymbol{yr}} \quad (5)$$

When determining the amount of pressure applied to each device, the average weight of each vehicle class was used to determine the weight of cars passing through the intersection, as shown in Table 2. It was assumed that for any given amount of time, an equal amount of vehicles of each class would pass through the intersection. An even distribution of vehicle class was used for simplicity, while still considering different weights of vehicles. Each vehicle was also assumed to hold two passengers, each with a weight of about 150 lbs or 650 N, with an even weight distribution across the four tires. Based on these assumptions, each of the four tires would

carry a load of 1049.25 lbs or 4781.19 N. Since the device dimensions are in metric units, metric weights will be used for the remaining analysis. Based on the dimensions of the devices and the approximate size of the impact area of a tire on a road (15 cm × 7.5 cm), each tire would contact about 60 input reservoirs at a time, meaning each device would see $1/60^{th}$ of the total weight applied at each tire. The impact area of a tire has a lot of variation based on the weight of the car and the tire pressure, so an estimated contact area was assumed in this analysis. To determine the amount of pressure applied to the devices, it was assumed that there was constant traffic moving through the intersection all day throughout the year. Based on these assumptions and the weight carried in each tire, each device would collect about 4.06 MPa, as demonstrated in Equation 6.

Table 2: Average curb weight of cars by vehicle class [17]

Vehicle Class	Curb Weight (lbs)	Curb Mass (kg)
compact car	2,979	1,354
midsize car	3,497	1,590
large car	4,366	1,985
compact truck/SUV	3,470	1,577
midsize truck/SUV	4,259	1,936
large truck/SUV	5,411	2,460

$$Pressure = \frac{F}{A} = \frac{\frac{1\ Tire}{60\ reservoirs} \times \frac{4781.19\ N}{Tire}}{\frac{\pi}{4}(0.005\ m)^2} = \frac{4{,}058{,}402.24\ \frac{N}{m^2}}{reservoir} \approx \boldsymbol{4.06} \frac{\boldsymbol{MPa}}{\boldsymbol{reservoir}} \quad (6)$$

The next part in this analysis is to determine how much flow is in the system to determine the power output of the devices. The expression for flow rate is listed in Equation 3 in Chapter 1. Since flow rate is dependent upon the channel dimensions, the number of channels, the pressure input, and the fluid properties, it can be calculated from all knowns at this point. For the no slip condition, the slip length is zero, however for the slip condition, the slip length is assumed to be

100 nm. The calculation of flow rate, Q, is shown below in Equation 7 where n is the number of channels connected in parallel. In this study, the kinematic viscosity of the solution is assumed to be equal to that of water at room temperature, 1.002×10^{-3} N-s/m^2. The no slip condition yields a flow rate of 1.01×10^{-13} m^3/s, while the slip condition yields a flow rate of 7.09×10^{-13} m^3/s. The values for flow rate are so small due to the nanoscale dimensions of the conduit. However, it is clear that the slip case yields much better results in flow rate, with an improvement of approximately seven times that of the no slip case, when using a 100 nm slip length.

$$Q = n\frac{-2wh^2\Delta P}{3\mu L}[h + 3b]$$
$$= 100\frac{-2(30 \cdot 10^{-6}m)(100 \cdot 10^{-9}m)^2(4.06 \cdot 10^6 Pa)}{3\left(1.002 \cdot 10^{-3}\frac{N \cdot s}{m^2}\right)(0.01m)}[100 \cdot 10^{-9} + 3b] \tag{7}$$

The final step in the analysis of the twelve-light traffic intersection is to compute the power output of the devices at a range of values of efficiency. The range of efficiency used to evaluate the cases is 30%, 50%, and 70% power conversion efficiency. These values were chosen because 30% is the maximum theoretical efficiency for a system with a 5 nm slip length, while 70% is the maximum theoretical efficiency for a 100 nm slip length [9]. The power output of the devices was calculated from rearranging the expression for power conversion efficiency as indicated below in Equation 8. The output values and percentages of the total light consumption are shown in Table 3.

.

$$P_{ext} = \varepsilon Q \Delta P \tag{8}$$

27

Table 3: Analysis of traffic lights in no slip and slip cases

Condition	ε	Consumption of 12 Traffic Lights (kW-hr/yr)	Power Output of Devices (kW-hr/yr)	% Light Consumption
No Slip	30%	1577	2.85	0.18
	50%	1577	4.75	0.30
	70%	1577	6.65	0.42
Slip	30%	1577	19.96	1.27
	50%	1577	33.26	2.11
	70%	1577	46.56	2.95

Based on the values presented in Table 3, the power outputs of this technology are very small as compared to the consumption of the LED traffic lights at the intersection. These results show that nanoP2P converters may not be feasible for large intersection applications. It is unknown how this results would scale to intersections of different size, so this would need further evaluation to determine the full extent of the feasibility of the traffic light application.

For the analysis of LED street lighting, many of the assumptions and calculations remained the same. The assumptions for this application differ from the traffic light case only by the amount and type of lights (one 25 W LED per streetlight) being powered by the nanoP2P converters. In this analysis, the same area of devices could be embedded under the pavement, spanning the width of the whole road. Assuming the same traffic conditions, the devices would generate the same about of power, however is supplied to only a single street light, since street lights are spread out along streets. Each streetlight operates 4100 hours per year, from dusk to dawn year round, and therefore the total consumption by a single 25 W light is 102.5 kW-hr annually. Therefore, this adjustment in power consumption greatly improves the results of the case study in this example. It can be seen in Table 4 that in the slip case, almost fifty percent of the light

consumption could be supplemented by nanoP2P devices, in optimal conditions. In a real situation, these devices would be connected to a series of capacitors that would store the power generated throughout the day. At dusk, the first couple hours of power could be supplied by the capacitors and in turn the nanoP2P converters.

Table 4: Analysis of street lighting in no slip and slip cases

Condition	ε	Consumption of 1 LED Street Light (kW-hr/yr)	Power Output of Devices (kW-hr/yr)	% Light Consumption
No Slip	30%	102.5	2.85	2.78
	50%	102.5	4.75	4.64
	70%	102.5	6.65	6.50
Slip	30%	102.5	19.96	19.46
	50%	102.5	33.26	32.43
	70%	102.5	46.56	45.40

3.2 Case Study II: Personal Devices

In order to evaluate the personal devices case study, some assumptions were made about the conditions of operation. The first assumptions made were that the average person weighs about 150 lbs or 650 N and that they are on their feet moving around throughout the day. The devices used in the case study had the same dimensions as in the last section. As mentioned in the previous chapter, it is known that the force applied is 1.5 times the bodyweight of a person when walking, and 3 times when running. It was also assumed that the heel of one foot and the toe of the other are in contact at the same time, such that half of the force is applied to each foot for ease of calculation and consistency between the walking and running cases. Additionally, the toe contains six devices while the heel contains only three devices, each area with equal pressure distribution as shown in Figure 10 in section 2.3 by the red input reservoirs. This means that

pressure is supplied to nine devices at all times, and in one shoe that force and pressure is distributed among six devices, but only three in the opposite shoe.

If an individual weighs near 650 N (150 lbs) and is walking, they are applying a force of 975 N (225 lbs) to their feet, and 1950 N (450 lbs) while running. With a reservoir diameter of 5 mm, each device in the toe of a shoe would experience 4.14 MPa from walking, and each heel would experience 8.28 MPa, as shown in Equations 9 and 10. In the running case, the pressure would double for both the heel and the toe yielding 8.18 MPa applied to the toe devices and 16.56 MPa to the heel devices. Using the no slip condition the flow rate was computed in each case and is listed below in Table 5.

$$Toe\ Pressure_{walking} = 1.5 \times \frac{650\ N}{person} \times \frac{person}{2\ shoes} \times \frac{shoe}{toe} \times \frac{toe}{6\ devices} \times \frac{device}{\frac{\pi}{4}(0.005m)^2} \quad (9)$$
$$= 4.14\ MPa$$
$$Heel\ Pressure_{walking} = 1.5 \times \frac{650\ N}{person} \times \frac{person}{2\ shoes} \times \frac{shoe}{heel} \times \frac{heel}{3\ devices} \times \frac{device}{\frac{\pi}{4}(0.005m)^2} \quad (10)$$
$$= 8.28\ MPa$$

Table 5: Computed flow rates for walking and running cases

Condition	Part of Shoe	ΔP (MPa)	Q (m³/s)
Walking	Heel	8.28	1.03×10^{-13}
	Toe	4.14	2.07×10^{-13}
Running	Heel	16.56	2.07×10^{-13}
	Toe	8.28	4.13×10^{-13}

Considering this power output per heel and toe for the walking scenarios, a power output for each condition and part of shoe was calculated with efficiencies varying from 30-70%. The summation of the heel and toe output powers are presented in Table 6 in the power output per person column. Only the no slip condition was analyzed in this case because the percent of smart

phone consumption was so low, that the improvements made by fluid slip would not make this application feasible.

Table 6: Analysis of nanoP2P converters with walking and running without fluid slip

Condition	ε	Consumption per Smart Phone (kW-hr/yr)	Power Output per Person (kW-hr/yr)	% Phone Consumption
Walking	30%	4.9	3.03×10^{-5}	6.19×10^{-4}
	50%	4.9	5.06×10^{-5}	1.03×10^{-3}
	70%	4.9	7.08×10^{-5}	1.44×10^{-3}
Running	30%	4.9	1.21×10^{-4}	2.48×10^{-3}
	50%	4.9	2.02×10^{-4}	4.13×10^{-3}
	70%	4.9	2.83×10^{-4}	5.78×10^{-3}

In review of the personal devices case study, it was determined that this application is not feasible with these devices. Only a small amount of devices could be embedded into a shoe in certain orientations due to size constraints. Although humans could exert a similar amount of pressure to the input reservoirs as seen in the traffic examples, this pressure is only supplied to nine devices at a time, yielding very small outputs of power. Therefore, it may be possible to utilize human movement in a different way that could incorporate more devices to generate more power.

Upon reflection of the case study results, another possible application of the nanoP2P converter was discovered. When applying a pressure around 85 psi, streaming potential outputs in the 1–100 nV range are expected. With such a small voltage output, it may be discovered that nanoP2P converters do not create enough energy to power devices. However, such a small output voltage introduces another opportunity for this technology: a finely-tuned pressure sensor. With relatively high pressure inputs, a very small voltage is measured across the nanochannel(s).

These devices could be implemented to sense small changes in pressure. Given the order of the voltage output, a change in just 1 psi should reflect a change in voltage, however the ratio between change in pressure and change in voltage is unknown. In order to accurately read such small fluctuations in voltage, a Faraday cage or other means of noise cancellation would be essential in producing accurate results. This is an application that needs further exploration and its own case study analysis, however it is worth noting that other applications may be available for this technology as well.

3.3 Test Setup Reliability

The reliability of the system needed to be validated a few different ways. The first was to ensure a leak-free system was built, without air leaks through the various connections and without solution leaks through the device. Air leaks would diminish the amount of pressure supplied to the device, and the full 85 psi would not be forcing ionic solution through the channel(s). Leaks of the ionic solution out of the channel or device would not provide accurate streaming potential feedback, and the efficiency of the device could not be properly analyzed. Example images capturing leaky channels and connections are provided below in Figure 17 and Figure 18, respectively.
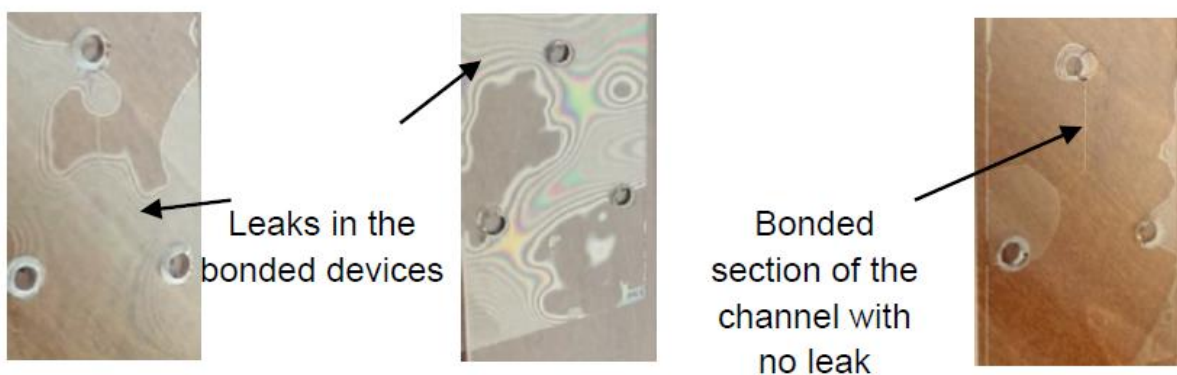

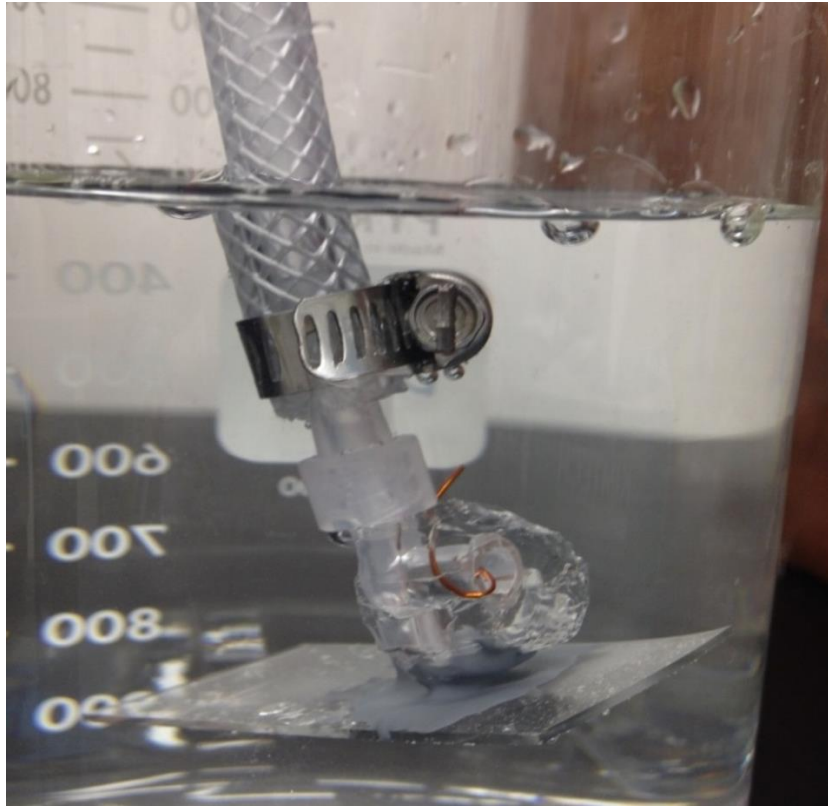Figure 17: Fluid leakage inside channels of bonded devices

Figure 18: Air leakage through epoxy at connector base

Trials were conducted in attempt to minimize leakage through the connections made in this setup. These trials entailed making PDMS caps around the T-connectors and allowing the caps to cure overnight, and then securing these connectors to devices with epoxy and allowing the epoxy to cure overnight again. Displayed below in Figure 19 through Figure 22 are a series of PDMS cap, connector, and device configurations. There were problems associated with each iteration that will be explained. In the first iteration, the epoxy connection was tested for effectiveness. However, in this case, the connector was bonded only to a glass slide with drilled holes and not a device with microchannels. This was done so that the bond could be tested without wasting an etched device which take several hours over the course of a few days to fabricate and bond. The epoxy connection was leak-free as demonstrated under water; however,

since the glass slide was open to the water through the bottom of the drilled hole, conclusions about the effectiveness of this bond could not yet be made.
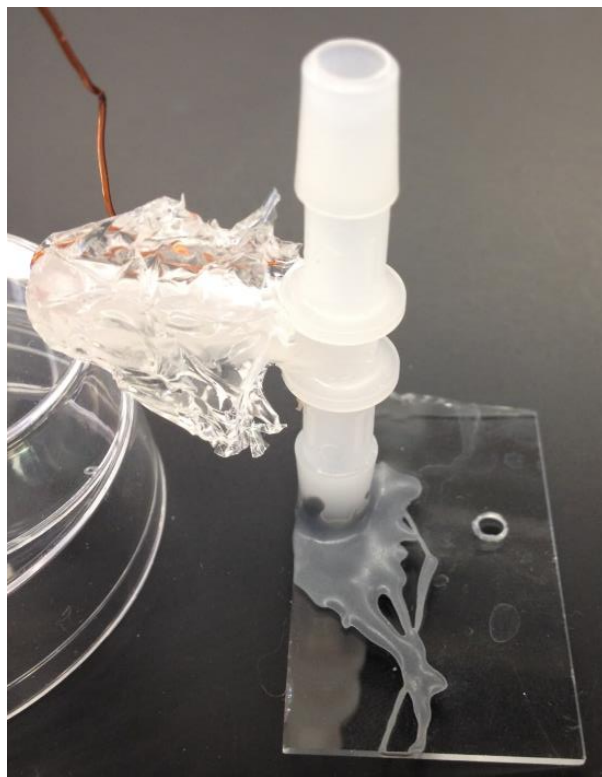

Figure 19: First iteration, T-connector secured to device by epoxy

In the remaining iterations, a different type of T-connector was used for easier assembly of the system. The Luer-Lock T-connector was implemented to allow the connector to screw into an adapter that fits with the tubing. This allows for the device to be attached to the tubing with a smaller risk of breaking the device from applying force to insert the connector into the tubing. This T-connector also made it much easier to feed the copper wire through the side arm and out the bottom of the connector because it has shorter arms compared to the previous T-connector. The epoxy connection with the device in the second iteration could not be evaluated because the device broke during assembly of the connector to the adapter. In the third iteration, the epoxy connection leaked under the PDMS cap. This occurred because the PDMS cap blocked access to

the entire diameter of the connector base, creating voids in the epoxy seal. Air leaked through these voids, creating a leaky system. In the fourth iteration, a smaller PDMS cap was created to allow access to the entire diameter of the connector base. A second connector was also added to the output reservoir to support the lead wire for data collection. With this final device, the connector shifted somewhat during application of the epoxy. The epoxy seemed to remain intact, however the connection was not leak-free as tested with applied air pressure the following day. The shift in the connector is believed to be the root cause for the leakage issues seen in this iteration.
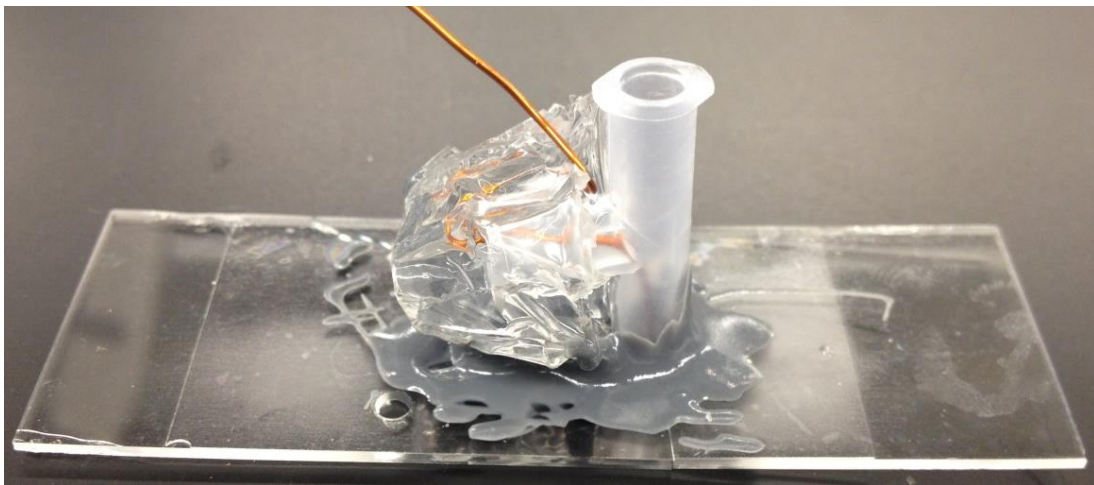

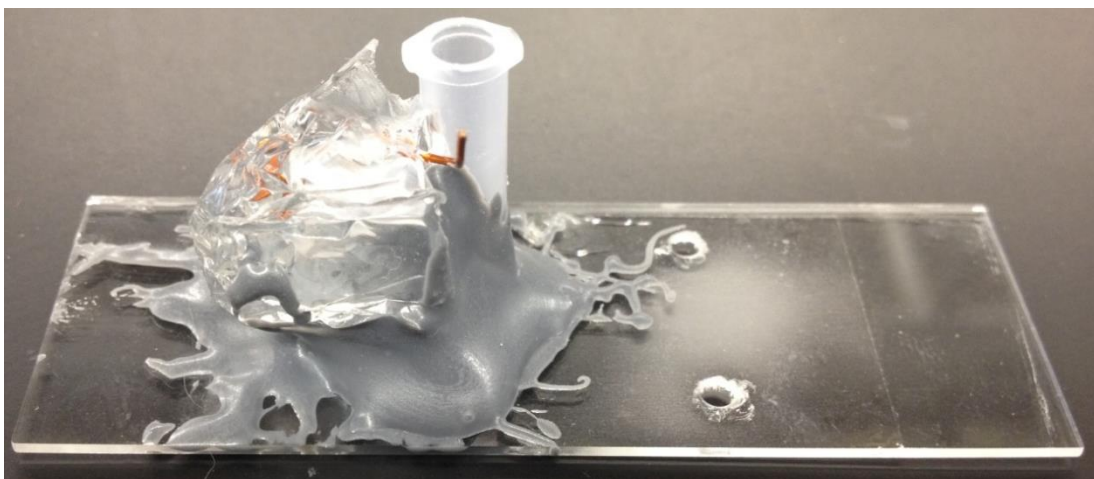Figure 20: Second iteration, T-connector secured to device by epoxy

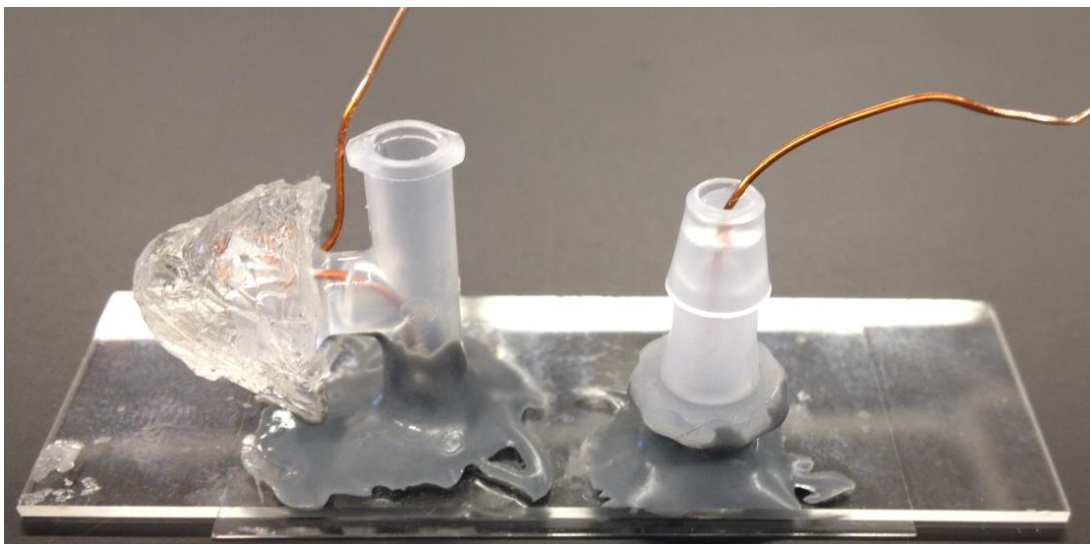Figure 21: Third iteration, T-connector secured to device by epoxy

35

Figure 22: Fourth iteration, T-connector secured to device by epoxy

During the multiple iterations of the connection trials for this research so far, different methods were used for supporting the connector. The first method utilized a ring stand to clamp to the PDMS cap and hold the connector above the device. This method yielded variable results and did not create an even force distribution on the connector or device. The ring stand did not hold the connector perfectly flat against the device, creating an imperfect seal with the epoxy. The second method of supporting the connector, as used in the fourth iteration, was to hold the connector vertically above the input reservoir in a vise. This method allowed for a more complete connection between the base of the connector and device, however it was more difficult to apply epoxy around the connector base due to the constraints of the vise walls.

Based on the results of the epoxy connections to the devices, it can be determined that design refinement will be necessary. First, it is difficult to align the T-connector perfectly with the reservoir to ensure complete contact. Second, it was challenging to support the T-connector while applying the epoxy without any shifting of the connector. Any movement of the connector while applying epoxy introduces the chance for a leaky connection or seepage of the epoxy into the reservoir. Epoxy in the reservoir could not only contaminate the solution, but could also

restrict flow through the channels and diminish efficiency or skew results. Third, it was difficult to ensure repeatable results while using epoxy because the secureness of the connection is unknown until the device is tested after the epoxy had cured for 24 hours. This introduces a large time delay and can attribute to wasted time in the process. Lastly, while the connector is being supported against the device during assembly, it is difficult to access the entire diameter of the base of the connector to obtain an even distribution of epoxy.

The second means of validating a reliable setup was to ensure a voltage was measured across the channel(s) and the values of the measurements seemed appropriate. In order to accomplish this portion of the validation process, voltage readings were planned to be collected at various pressure inputs to ensure that a different voltage resulted from differing pressures. However, in normal operation of this system, 85 psi would be applied to the system to force solution through the channels for comparison to existing research in this field. This data collection process was unsuccessful because a perfectly leak-free system was not obtained. Data collection was attempted with a leaky epoxy connection, however it appeared that the ionic solution did not enter the channel from the input and output reservoirs. This could mean that there was an obstruction in the flow of the solution in the reservoir. This obstruction could have resulted from a contaminant entering the device through the connector or there could have been a small amount of epoxy obstructing flow that was not visible from the outside of the device. Since there was no flow of solution through the channel, no data could be collected from the device. Images of the test station setup are displayed below in Figure 23, showing the entire setup and detail of the connections inside the Faraday cage. The Faraday cage was used in the setup because the expected voltage outputs were in the range of 1–100 nanoVolts, so any noise from outside sources could impact readings.
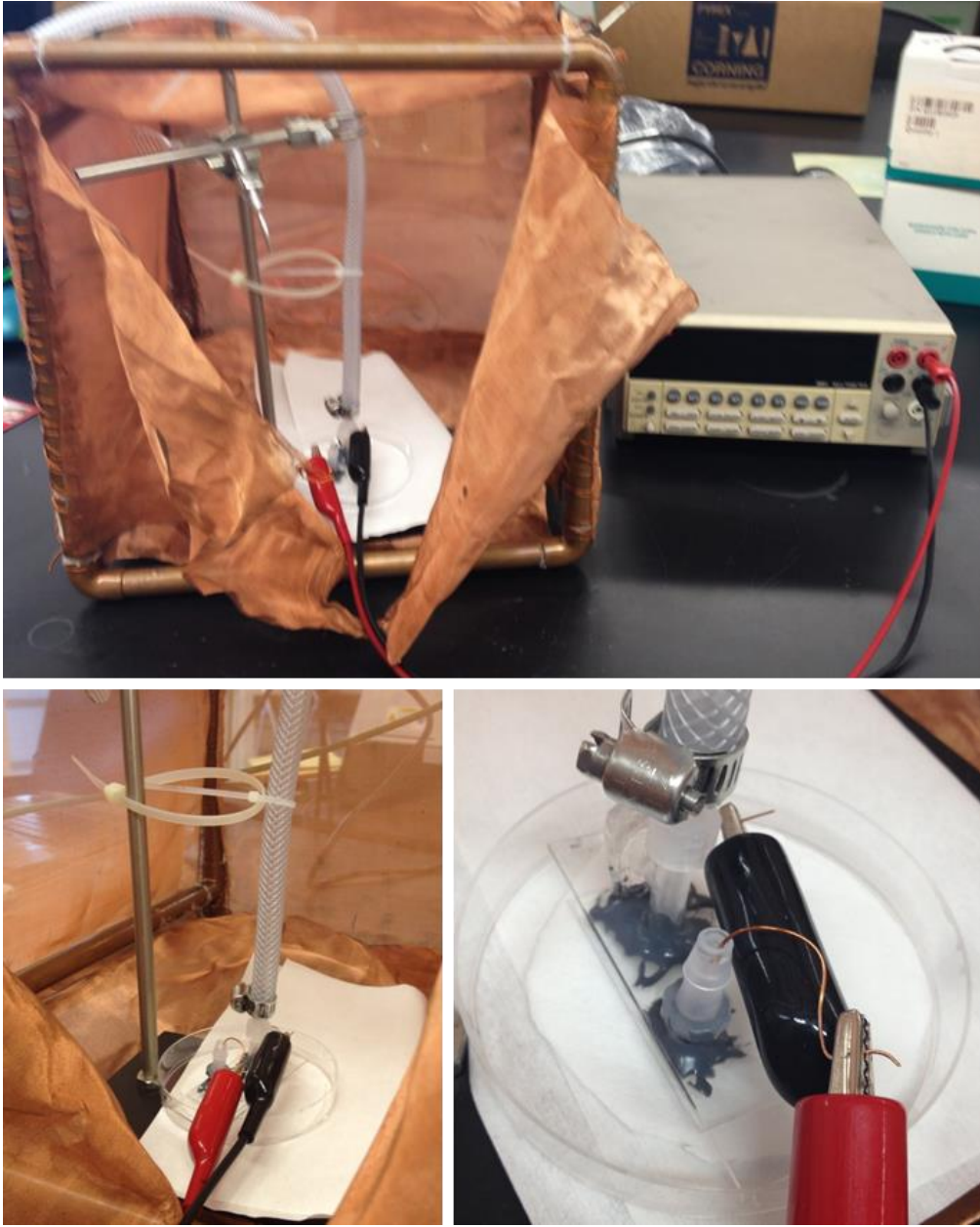
Figure 23: Test station setup

CHAPTER 4: CONCLUSIONS AND FUTURE WORK

In this Honor's Undergraduate Thesis, the feasibility of nanoP2P converters was investigated for three case studies and a test setup was built to test the energy conversion ability nanoP2P converters. Based on the case studies presented here, it was determined that nanoP2P converters would not supply enough energy to power or supplement large traffic intersections. However, smaller traffic intersections still need to be evaluated. It is unclear how the results would scale with varying intersections sizes. This technology seems capable of supplementing the electricity supplied to streetlights. Nearly fifty percent of the power consumption could be supplied by nanoP2P converters in optimal conditions. In review of the personal devices case study, it was determined that this application is not feasible in the no slip condition due to the small theoretical output powers and percentages of smart phone consumption. Analysis yielding optimal design parameters needs to be conducted to determine the appropriate dimensions and slip length of the device for highly efficient power conversion. Additional case study analyses need to be performed to discover further applications that included both a source of waste pressure and an applicable technology to power with the converted energy. Lastly, it remains unknown if nanoP2P converters could operate as pressure sensors.

This thesis also served to create a reliable test station that could evaluate nanoP2P converters. The setup was built as designed, however under high pressure the epoxy connections did not hold. Small audible and visible leaks were observed; however, connections were not blown off and the epoxy remained intact after the device was disconnected from a pressure of 85 psi. This demonstrated that the epoxy itself makes a strong connection, however it is difficult to obtain an entirely sealed connection with this method. The evaluation of the setup showed that the device could supply a large pressure without leakage through the PDMS cap or the T-

connector and tubing interface; however, a perfect epoxy connection could not be obtained at the operating pressure of 85 psi.

The future work for this research will be carried out over the next year as a Master's student in the Mechanical Engineering program at The Ohio State University. The first step would be to continue developing and analyzing new case studies to find more appropriate applications of this technology. Along with the case study analysis, the design parameters need to be studied and analyzed in greater depth to determine the optimal parameters for operation. The next step would be to make design changes that could yield more repeatable results in terms of the connections made between components.

After the test setup is fully functional, nanoP2P converters will be designed and fabricated with substrate properties that demonstrate a highly efficient device and advance the state-of-the-art. The properties to optimize include surface charge density of the substrate and engineering slip into the system. Surface charge densities impact ionic attraction to the walls of the channel and alter the amount of streaming current generated inside the channels. Fluid slip, as demonstrated in the case study analysis, improves the flow rate inside the channels greatly and therefore improves power generation. There is an unknown balance that allows for optimal surface charge density and slip to maximize the power conversion efficiency, which will be investigated next year. In order to alter surface charge densities and induce fluid slip, chemical compounds which alter the surface properties will be bonded to the surface of the nanochannel walls. The synthetic chemistry method known as "click" chemistry will be used to bond compounds to the substrate [17]. The final step in continuation of this project would be to develop a program to collect streaming potential, streaming current, pressure, and flow rate data and evaluate the system for power conversion efficiency. The ultimate goal is for this research is

to be the first to demonstrate the effectiveness of nanoP2P converters with altered surface properties of the substrate by engineering both fluid slip and surface charge density.
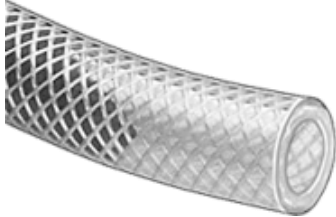
REFERENCES

[1]   Unites States. Energy Information Administration. Independent Statistics and Analysis. *Total Energy Overview*. By EIA. N.p., 2014.

[2]   "Why are they replacing all of the traffic lights in my town?" 01 April 2000. HowStuffWorks.com.

[3]   Tweed, Katherine. "Cree Launches $99 LED Street Light." Greentechmedia. N.p., 6 Aug. 2013.

[4]   Collins, Jeff. "Fracking Awesome." Nchouse25.com. N.p., 20 Aug. 2014.

[5]   Hegar, Glenn. "Biodiesel." The Energy Report. Golden, CO: National Renewable Energy Laboratory, 2008. 211-26. Texas Comptroller of Public Accounts. May 2008.

[6]   Li, Deyu. "Nanochannel Fabrication." Encyclopedia of Microfluidics and Nanofluidics (2008): 1409-414. Springer US.

[7]   Heyden, Frank Van Der, Derek Stein, and Cees Dekker. "Streaming Currents in a Single Nanofluidic Channel." Physical Review Letters 95.11 (2005): n. pag.

[8]   Olthuis et al. "Energy from Streaming Current and Potential." Sensors and Actuators B: Chemical 111-112 (2005): 385-89.

[9]   Pennathur, S., Eijkel, J. C., & Van den Berg, A. (2007). Energy conversion in microsystems: Is there a role for micro/nanofluidics? *Lab on a Chip, 7*(10), 1234-1237.

[10]   Federal Highway Administration. "Frequently Asked Questions – Part 4 – Highway Traffic Signals." Manual on Uniform Traffic Control Devices (MUTCD). U.S. Department of Transportation, 2015.

[11]   International Dark-Sky Association. "Economic Issues in Wasted and Inefficient Outdoor Lighting." Information Sheet no. 26.

[12] "Number of Smartphone Users in the U.S. from 2010 to 2018 (in Millions)." Statista.

[13]   Fischer, Barry. "How Much Does It Cost to Charge an IPhone 5? A Thought-provokingly Modest $0.41/year." Web log post. Outlier. Opower, 27 Sept. 2012.

[14] Apple Inc. "IPhone 5 - Technical Specifications." IPhone 5 - Technical Specifications. Apple Inc., 24 Oct. 2013.

[15] Samsung Electronics Co. "Specifications: Samsung GALAXY S3." Samsung GALAXY S3. Samsung Electronics Co, 2013.

[16] Lieberman, Daniel E., Madhusudhan Venkadesan, Adam I. Daoud, and William A. Werbel. "Biomechanical Differences Between Different Foot Strikes." Running Barefoot: Biomechanics of Foot Strike. Harvard University, 2010.

[17] Woodyard, Chris. "Vehicles Keep Inching up and Putting on Pounds." USATODAY.com. USA TODAY, 16 July 2007.

[18] Prakash, S., Long, T. M., Selby, J. C., Moore, J. S., & Shannon, M. A. (2007). "Click" Modification of Silica Surfaces and Glass Microfluidic Channels. Analytical Chemistry, 79(4), 1661-1667.

APPENDIX A

Test Setup Components

	Stainless Steel Hose Coupling
	    • Max Pressure: 300 psi
	    • Image and specifications from McMaster-Carr

	High-Pressure Tygon PVC Tubing
	    • Max Pressure: 250 psi
	    • ID: ¼"
	    • Image and specifications from McMaster-Carr

	White PVDF Barbed Tube Fitting
	    • Max Pressure: 150 psi
	    • Image and specifications from McMaster-Carr

	Breeze Mini Hose Clamps
	    • Secure pipe to connector at various joints
	    • Image from Breeze Hose Clamps

	Polydimethylsiloxane (PDMS)
	    • Seal arm of T-connector with lead wire
	    • Image from Elveflow, "PDMS: A Review"

	Double-Bubble Epoxy, Orange Package
	    • Seal T-connector to device input reservoir
	    • Tensile Strength: 250 psi
	    • Image and specifications from Royal Adhesives